Spatial Distribution of Maxi-Anion Channel on Cardiomyocytes Detected by Smart-Patch Technique

Amal K. Dutta,* Yuri E. Korchev,† Andrew I. Shevchuk,† Seiji Hayashi,* Yasunobu Okada,* and Ravshan Z. Sabirov*‡

*Department of Cell Physiology, National Institute for Physiological Sciences, Okazaki 444-8585, Japan; †Division of Medicine, Imperial College London, Medical Research Council Clinical Sciences Center, Faculty of Medicine, London SW3 6LY, United Kingdom; and ‡Department of Biophysics, National University of Uzbekistan, Tashkent 700174, Vuzgorodok, Uzbekistan

ABSTRACT Spatial distribution of maxi-anion channels in rat cardiomyocytes were studied by applying the recently developed patch clamp technique under scanning ion conductance microscopy, called the ''smart-patch'' technique. In primary-cultured neonatal cells, the channel was found to be unevenly distributed over the cell surface with significantly lower channel activity in cellular extensions compared with the other parts. Local ATP release, detected using a PC12 cell-based biosensor technique, also exhibited a similar pattern. The maxi-anion channel activity could not be detected in freshly isolated adult cardiomyocytes by the conventional patch-clamp with 2-MΩ pipettes. However, when fine-tipped 15–20 MΩ pipettes were targeted to only Z-line areas, we observed, for the first time, the maxi-anion events. Smart-patching different regions of the cell surface, we found that the channel activity was maximal at the openings of T-tubules and along Z-lines, but was significantly decreased in the scallop crest area. Thus, it is concluded that maxi-anion channels are concentrated at the openings of T-tubules and along Z-lines in adult cardiomyocytes. This study showed that the smart-patch technique provides a powerful method to detect a unitary event of channels that are localized at some specific site in the narrow region.

INTRODUCTION

The maxi-anion channel has been observed in a wide variety of cell types and exhibits roughly uniform behavior (1,2), suggesting it has a general physiological function. We have determined recently that the maxi-anion channel is a nanoscopic pore (3) well-suited to function as an ATP-releasing pathway (2,4). This pore accounts for the swelling-induced ATP release from mouse mammary C-127 cells (5,6) and NaCl-dependent ATP-mediated signaling from macula densa cells to mesangial cells during tubuloglomerular feedback in the kidney (7).

In the heart, many subtypes of ionotropic P2X receptors and metabotropic P2Y receptors are expressed (8), and a variety of effects of extracellular ATP on the heart have been reported (9,10). There are a number of possible sources of cardiac ATP release. These include purinergic nerves innervating the heart (11), cardiac vascular endothelial cells (12), and cardiomyocytes themselves (13). In our previous study (14), it was shown that neonatal rat cardiomyocytes in primary culture respond to ischemic/hypoxic stress as well as to a hypotonic challenge with the massive release of ATP and activation of single-channel events with a large unitary conductance (~390 pS). The channel was selective to anions, showed significant permeability to ATP^{4-}, and exhibited pharmacological properties essentially identical to those of ATP release. Based on these findings, we concluded that the ATP release from neonatal rat cardiomyocytes is mainly mediated by activity of the maxi-anion channel under ischemic or hypotonic conditions (14).

Paradoxically, these channels could not be observed in cardiomyocytes freshly isolated from adult hearts with commonly used patch-clamp conditions (14,15). It was therefore suggested that maxi-anion channels are only transiently expressed in neonatal cells, disappearing on maturation (15). However, ATP release from mature cardiomyocytes (13) and purinergic signaling in the normal and diseased heart (8–10) are well-recognized phenomena. We thus hypothesized that the difference in maxi-anion channel activity between neonatal and adult cells could be related to different pattern of spatial distribution of the maxi-anion channels over the surface of sarcolemma. In this study, the spatial distribution of maxi-anion channels and that of ATP release site were first studied in neonatal rat cardiomyocytes by using a smart-patch method and an ATP biosensor technique, respectively. The finding that both distributions match with each other provides further evidence for the ''maxi-anion channel = ATP-conductive channel'' concept. We then reexamined functional expression of maxi-anion channels in adult rat cardiomyocytes by the smart-patch method using very fine-tipped patch pipettes. We show, for the first time, that in adult cells, the maxi-anion channel activity is localized only at specific sites of the plasma membrane associated with the T-tubular system and Z-lines.

Submitted July 20, 2007, and accepted for publication October 24, 2007.

Address reprint requests to Y. Okada, Department of Cell Physiology, National Institute for Physiological Sciences, Myodaiji-cho, Okazaki 444-8585, Japan. Tel: 81-564-55-7731, Fax: 81-564-55-7735, E-mail: okada@nips.ac.jp.

Editor: Richard W. Aldrich.

0006-3495/08/03/1646/10 $2.00

doi: 10.1529/biophysj.107.117820

MATERIALS AND METHODS

Cells

The experimental protocols were approved in advance by the Ethics Review Committee for Animal Experimentation of the National Institute for Physiological Sciences. Neonatal rat cardiomyocytes were prepared from ventricles isolated from 2- to 3-day-old Wistar rats (Japan SLC, Shizuoka Laboratory Animal Center, Shizuoka, Japan) after decapitation, according to the method described previously (14,16). Cells were cultured in M199 medium supplemented with 10% newborn bovine serum in 35-mm culture dishes for 1 h. Nonadherent cells (mostly cardiomyocytes) were plated on collagen-coated glass cover slips and then cultured for 2–3 days. Scanning ion conductance microscope (SICM) cell imaging and patch-clamp experiments were carried out when the cell density reached 3×10^3 cell/cm^2.

Single adult ventricular myocytes were isolated from male Wistar rats (7–9 weeks), as described previously (17). Briefly, hearts were quickly isolated from rats anesthetized with pentobarbital (Abbott Laboratories, North Chicago, IL) and put into ice-cold, Ca^{2+}-free, modified Tyrode solution composed of (in mM): 133.5 NaCl, 4 KCl, 1.2 $MgSO_4$, 1.2 NaH_2PO_4, 10 HEPES, and 11 glucose (pH 7.4 adjusted with NaOH). The aortas were cannulated and mounted on a Langendorff apparatus at 37°C. The hearts were perfused for 5 min with Ca^{2+}-free Tyrode solution saturated with 100% O_2 and subsequently, for 20–30 min with the same solution containing bovine serum albumin (1 mg/ml) and collagenase S-1 (0.15 mg/ml; Nittazeratin, Osaka, Japan) or collagenase (0.15 mg/ml; Yakult, Tokyo, Japan). The ventricles were minced in KB solution containing (in mM): 70 L-glutamic acid, 25 KCl, 20 taurine, 10 KH_2PO_4, 3 $MgCl_2$, 0.5 EGTA, 10 glucose, and 10 HEPES (pH 7.4 with NaOH). The cell suspensions were stored in KB solution at room temperature (22–26°C) and used for experiments within 6 h.

PC12 cells were obtained from Riken Cell Bank (Tsukuba, Japan), cultured in DMEM supplemented with 10% FCS, and used for patch-clamp experiments without induction of neuronal differentiation.

Solutions and chemicals

For scanning and patch-clamp experiments cells were bathed with NMDG-Cl or TEA-Cl solution containing (mM): 140 NMDG-Cl or TEA-Cl, 1 $MgCl_2$, 11 HEPES, 5 glucose, and 1 EGTA (pH 7.4 adjusted with NMDG or TEA-OH, 290 mosmol (kg H_2O)$^{-1}$). Pipette TEA-Cl or NMDG-Cl solution contained (mM): 140 TEA-Cl or NMDG-Cl, 2 $CaCl_2$, 1 $MgCl_2$, 5 Na-HEPES, 6 HEPES, and 5 glucose (pH 7.4, 290 mosmol (kg H_2O)$^{-1}$). For measurements of relative permeability, both NaCl and KCl in the Ringer solution were replaced with NMDG-Cl, or NaCl was replaced with Na-glutamate. In some experiments, cells were bathed and pipettes were filled with Ringer solution containing (mM): 135 NaCl, 5 KCl, 2 $CaCl_2$, 1 $MgCl_2$, 5 Na-HEPES, 6 HEPES, and 5 glucose (pH 7.4, 290 mosmol (kg H_2O)$^{-1}$). The pipette solution used for whole-cell recordings in biosensor PC12 cells contained (mM): 125 CsCl, 2 $CaCl_2$, 1 $MgCl_2$, 5 HEPES (pH 7.4 adjusted with CsOH), and 10 EGTA (pCa 7.6; 275 mosmol (kg H_2O)$^{-1}$). Hypotonic bath solution for cell-attached experiments contained (mM): 100 NaCl, 5 KCl, 1 $MgCl_2$, 5 Na-HEPES, 6 HEPES, 5 glucose, and 1 EGTA (pH 7.4 adjusted with NaOH, 215 mosmol (kg H_2O)$^{-1}$). The isotonic bath solution for cell-attached experiments was made from the hypotonic solution by adding an appropriate amount of mannitol.

5-Nitro-2-(phenylpropylamino)-benzoate (NPPB), 4-acetamino-4′-isothiocyanostilbene (SITS) and arachidonic acid were purchased from Sigma-Aldrich (St. Louis, MO) and were added to the test solution immediately before use from stock solutions in DMSO. DMSO did not have any effect, when added alone at a concentration <0.1%. $GdCl_3$ was stored as a 50-mM stock solution in water and added directly to the test solution immediately before each experiment. Apyrase was purchased from Yakult.

Osmolality of all solutions was measured using a freezing-point depression osmometer (OM802, Vogel, Kevelaer, Germany).

Conventional patch-clamp recordings

Patch electrodes, fabricated from borosilicate glass using a micropipette puller (P-97, Sutter Instrument, Novato, CA), had a tip resistance of ~2 MΩ for whole-cell current measurements and for some single-channel recordings, 7–20 MΩ for single-channel recordings, when filled with pipette solution. For whole-cell recordings, the access resistance did not exceed 5 MΩ and was always compensated for (by 70–80%). Membrane currents were measured with an Axopatch 200A patch-clamp amplifier coupled to a DigiData 1322A interface (Axon Instruments, Union City, CA). Currents were filtered at 1 kHz and sampled at 2–5 kHz. Data acquisition and analysis were done using pCLAMP 8.1 (Axon Instruments) and WinASCD software (kindly provided by Dr. G. Droogmans, KU Leuven, Belgium).

Whenever the bath chloride concentration was changed, a salt bridge containing 3 M KCl in 2% agarose was used to minimize bath electrode potential variations. The liquid junction potentials were calculated using pCLAMP8 algorithms and corrected when necessary.

High-resolution scanning patch-clamp technique

The basic arrangement and operation of the SICM have been described previously (18–22). In this study, we used a similar set-up. Briefly, a fine-tipped 80–100-MΩ pipette, called a nano-pipette (21), was used as a probe to image the surface topography of myocytes (Fig. 1 *A*). In some experiments, a

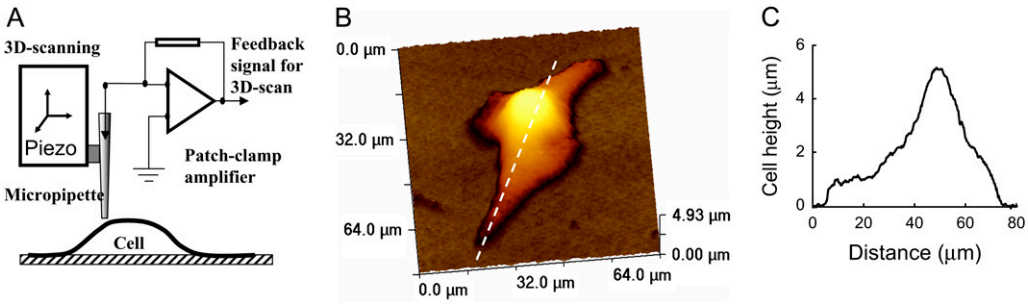

FIGURE 1 SICM imaging of a cultured cardiomyocyte. (*A*) Schematic diagram of the SICM technique. The micropipette is mounted on a three-axis piezo actuator (not shown) controlled by a computer. The ionic current that flows through the pipette is measured by a patch-clamp amplifier, and is used for feedback control that allows the maintenance of a constant distance between the micropipette and the sample during scanning. After 3D images are taken, computer control is used to position the micropipette at a place of interest based on the topographic image acquired, and the same patch-clamp amplifier is used for single-channel recordings. (*B*) 3D image of a cultured rat cardiomyocyte. The integrated cell volume is 1887 μm^3. (*C*) Variation of the cell surface height along a line (white line shown in *B*) drawn through the center of the cell. The peak height for this particular cell was 4.5 μm.

relatively wide-tipped micropipette of 20–35 MΩ was used. The electrode was connected to an Axopatch 200A patch-clamp amplifier coupled to a DigiData 1322A interface (Axon Instruments). The probe was mounted on a piezo translation stage (Tritor, Piezosystem Jena, Germany) that is modulated vertically 40 nm at 200 Hz (23). The modulated current was amplified and fed to a DSP card (M44 TMS320C44 DSP board equipped with A4D4 AD/DA converter, Innovative Integration, CA) that generated the feedback signal used to maintain the probe-sample separation distance. To scan the specimen the nanopipette probe was driven in the *x*- and *y*-directions by the electronics. The information on both the lateral and vertical positions was recorded and used to generate the three-dimensional (3D) topographic image. SICM Imaging software for DSP card together with image analysis software was provided by the Ionscope Ltd. (London, UK).

The coordinates of the SICM images were used subsequently for precise positioning of the pipette on a defined area of interest on the cell surface. This method is known as a high-resolution scanning patch-clamp or smart patch-clamp (22). A patch pipette was vertically placed and lowered by piezo control until contact with the cell surface, usually after moving it down by one tip radius. To reach into the T-tubule region, a downward movement of ~2 μm was required. Light suction was necessary to form a GΩ seal. A tight seal with a resistance of ~10 GΩ was routinely maintained in cell-attached recordings. Currents were filtered at 1 kHz and sampled at 2–5 kHz. Data acquisition and analysis were done using pCLAMP 8.1 (Axon Instruments) and WinASCD software (kindly provided by Dr. G. Droogmans, KU Leuven, Belgium). Whenever the bath chloride concentration was changed, a salt bridge containing 3 M KCl in 2% agarose was used to minimize bath electrode potential variations.

Detection of ATP release by a biosensor technique

A biosensor method (24,25) was used to measure the local concentration of ATP released from a single cardiomyocyte. Whole-cell currents were recorded from a PC12 cell, which expresses P2X receptor channels, at a holding potential of −50 mV, before and after placing the biosensor cell on different areas of the cardiomyocyte. The current responses were observed on changing the bath solution to a hypotonic one. In some experiments, effects of high-K^+-induced depolarization were observed by replacing the bath solution with isotonic high K^+ solution containing (in mM): 105 KCl, 1 $MgCl_2$, 5 Na-HEPES, 6 HEPES, 5 glucose, and 1 EGTA (pH 7.4, 290 mosmol (kg H_2O)$^{-1}$ adjusted with mannitol). For calibration experiments, ATP was applied to a PC12 cell without positioning the biosensor cell near a cardiomyocyte, through a micropipette filled with an ATP-containing bath solution (for details see (25)). The ATP-induced currents were detectable at concentrations >1 μM, and the half-maximal concentration was 30.4 ± 2.9 μM, as reported previously (7,24,25). Because the ATP-induced P2X receptor current was sensitive to SITS and Gd^{3+}, it was not possible to use these drugs in the biosensor assay.

Data analysis

Single-channel amplitudes were measured by manually placing a cursor at the open and closed channel levels. Background currents were subtracted, and the patch currents were measured at the beginning (first 25–30 ms) of current traces to minimize the contribution of voltage-dependent current inactivation. By dividing the mean patch current by the single-channel amplitude, the mean number of open channels, NP_o, was calculated, where P_o and N represent the open channel probability and the number of active channels, respectively. The single-channel current-voltage (I/V) relationships in asymmetric conditions were fitted to a second-order polynomial and reversal potentials were calculated as described previously (3). The permeability ratio for glutamate to chloride was calculated using the Goldman-Hodgkin-Katz (GHK) equation, as described previously (3).

Data were analyzed in Origin 6 and OriginPro 7.0 (MicroCal Software, Northampton, MA). Pooled data are given as mean ± SE of observations (*n*). Statistical differences of the data were evaluated by ANOVA and the paired or unpaired Student's *t*-test where appropriate, and considered significant at $p < 0.05$.

In all figures, the membrane potential (V_m) is denoted according to the following convention: $V_m = V_p$ (the pipette potential) for whole-cell, and $V_m = -V_p$ for inside-out, experiments. For on-cell records, applied voltages represent $-V_p$ values.

All experiments were carried out at room temperature (23–25°C).

RESULTS

Distribution of maxi-anion channels over the cell surface of cultured neonatal rat cardiomyocytes

To determine the distribution of maxi-anion channel activity over the surface of cultured neonatal rat cardiomyocytes, we first imaged the cells using the SICM technique (Fig. 1 *A*). Fig. 1 *B* shows an example of such an image. In normal conditions, the cultured cardiomyocytes had a relatively high central hill-like cell body surrounded by spreading edges or extensions. The cell volume of single cardiomyocyte was equal to 1783 ± 145 μm^3 ($n = 15$), corresponding to a radius of 7.5 μm. The capacitance (8.1 ± 0.9 pF; $n = 6$) measured from single detached cardiomyocytes in the conventional whole-cell mode was close to the value (7.1 pF) calculated by the cell surface area assuming a specific membrane capacitance of 1 $\mu F/cm^2$. Fig. 1 *C* shows the variation of cell surface height along a line (white line shown in Fig. 1 *B*) drawn through the center of the cell. The height of the cells varied in a range from 3.1 to 10.3 μm. The mean cell height was 5.9 ± 0.2 μm (averaged from 64 different cultured cardiomyocytes). In the following experiments, the same patch pipette was used to sequentially image the cells by SICM and then to patch specified regions on the cells (a smart-patch technique). We classified the total cell surface into three different parts (see Fig. 2 *A* for definitions): 1), the surface of the center of the cell, defined as the surface located in the region within 10% of the vertical distance from the top of the cell; 2), the peripheral surface, located in the region between 10% of the vertical distance from the top and 20% from the bottom of the cell; and 3), the surface of extensions, located at the bottom of the cell and not in the area above 20% of the total cell height.

Similar to our previous observations (14), the maxi-anion channel was inactive in the cell-attached mode but readily activated on patch excision. Maxi-anion channel activity was found in inside-out patches excised from all three areas of the surface. Fig. 2 *B* shows current traces recorded from the membrane patches with the same pipette used for 3D images. The observed single-channel current amplitude was 18.3 ± 0.6 pA at +50 mV and −18.8 ± 0.7 pA at −50 mV when recordings were made from the cell center. Similarly, channel currents of 18.6 ± 0.4 pA at +50 mV and 18.8 ± 0.7 pA at −50 mV were recorded from the peripheral surface. The single-channel amplitude of currents recorded from cell extensions was 18.1 ± 1.1 pA at +50 mV and –18.3 ± 0.7 pA at −50 mV. The single-channel current amplitudes did not significantly

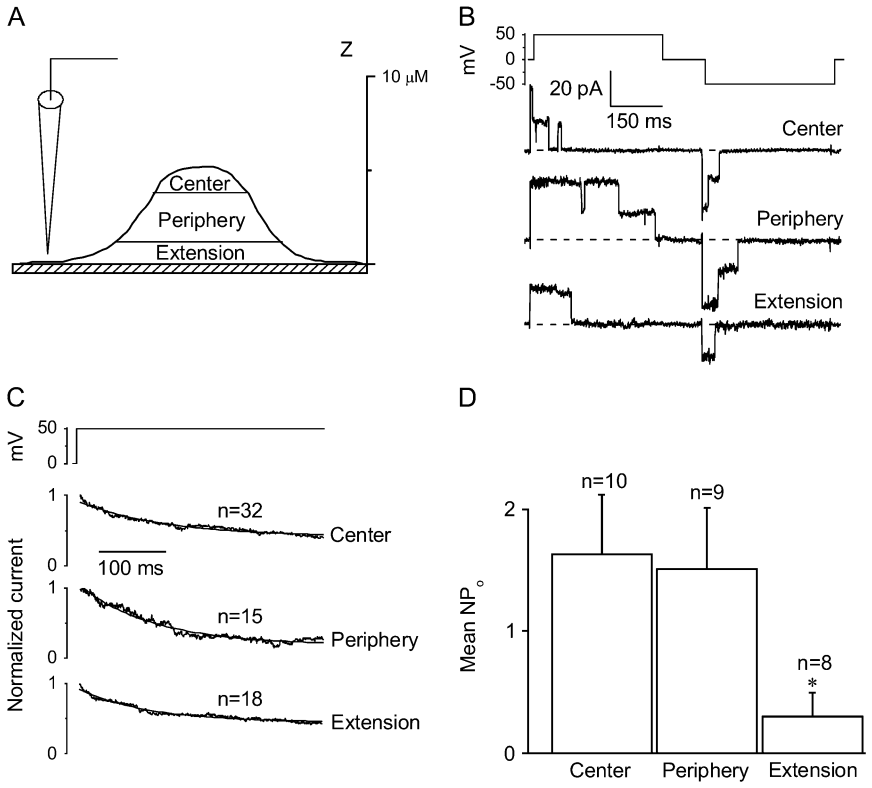

FIGURE 2 Spatial distribution of maxi-anion channels over the sarcolemma of cultured rat cardiomyocytes. (*A*) Schematic diagram representing the areas for single-channel recording in the sarcolemma of a rat cardiomyocyte. (*B*) Representative single-channel current traces recorded during application of alternating step-pulses to ±50 mV (the protocol shown at the top of the traces), from patches excised from the central (*top trace*), peripheral (*middle trace*) and extension (*bottom trace*) regions of a cell. (*C*) Kinetics of inactivation of single maxi-anion channels. Ensemble averaged currents were obtained in response to consecutive applications of depolarizing step-pulse of +50 mV (the protocol shown at the top of the traces); *n* represents the number of records used for averaging. Solid lines are single-exponential fits with a time constant of 132.8 ± 3.3 ms, 113.8 ± 2.4 ms, and 107.4 ± 2.2 ms for the central (*top trace*), peripheral (*middle trace*), and extension (*bottom trace*) regions, respectively. (*D*) Mean maxi-anion channel activity (expressed as NP_o) in the different regions of cultured cardiomyocytes. Each column represents the mean ± SE (vertical bar). *Significantly different at $p < 0.05$ vs. center.

differ from each other when tested by ANOVA. Single-channel inactivation kinetics on application of depolarizing step-pulses to +50 mV were not notably different between different areas that exhibit the time constants of ~100–130 ms (Fig. 2 *C*). In contrast, maxi-anion channel activity, expressed as the mean NP_o value, was not distributed evenly between the different areas of the cell surface. The mean NP_o value was significantly lower at the cell extensions compared with the central and peripheral parts of the cell surface (Fig. 2 *D*).

Swelling-induced ATP release from specific regions of the cell surface of cultured neonatal rat cardiomyocytes

In previous studies, we have shown that the maxi-anion channel serves as a conductive ATP-releasing pathway in a number of cell types (5–7) including neonatal rat cardiomyocytes (14). If the channel activity is unevenly distributed over the cell surface, we might expect a similarly uneven variation in the efficiency of ATP release. To measure the local concentration of released ATP in different parts of the sarcolemma, we used a P2X-receptor-based biosensor technique (24,25). In these experiments, as depicted in Fig. 3 *A*, we monitored the cells under a high-resolution inverted microscope and placed the PC12 biosensor cell in close proximity to (often touching) areas approximately the same as those used in smart-patch experiments. Fig. 3 *B* shows a series of inward current spikes recorded from a PC12 cell touching locations in the central, peripheral, and extension areas of cultured cardiomyocytes, on exposure to a hypotonic stimulation. The ATP-evoked current responses from the cell center and periphery were detected after lag periods of 3.0 ± 1.1 and 3.1 ± 1.5 min, respectively ($n = 5$–6); these values are close to what we observed previously (14). In contrast, no statistically significant inward current spikes were observed over a recording time of ~20 min, when PC12 cells were positioned at the cell extensions (Fig. 3 *B, bottom trace*). Inward current responses disappeared when the voltage-clamped PC12 cell was moved apart from the cardiomyocyte. As we described in our previous study (14), these inward currents were markedly suppressed when hypotonic solution was supplemented with a P2-receptor blocker, suramin (300 μM), or an ATP-hydrolyzing enzyme, apyrase (0.1 mg/ml), suggesting that the currents were activated by the released ATP. Consistent with our previous studies (14,24), no current responses were detected for a PC12 cell alone, exposed to hypotonic solution without positioning near a cardiomyocyte ($n = 4$). Fig. 3 *C* summarizes the mean peak current density for different areas of the cardiomyocyte surface membrane. The density of the ATP-evoked current was significantly lower for cell extensions compared with the central and peripheral areas of the cell surface. Using the measured biosensor current densities and a calibration curve (see Materials and Methods), we estimated the local ATP concentration to be 23.5 ± 8.0 μM, 21.2 ± 8.5 μM, and 1.4 ± 0.6 μM for the central, peripheral and extension regions of the cell surface, respectively. Thus, it seems that the spatial distribution of ATP release site matches with that of maxi-anion channels in neonatal rat cardiomyocytes.

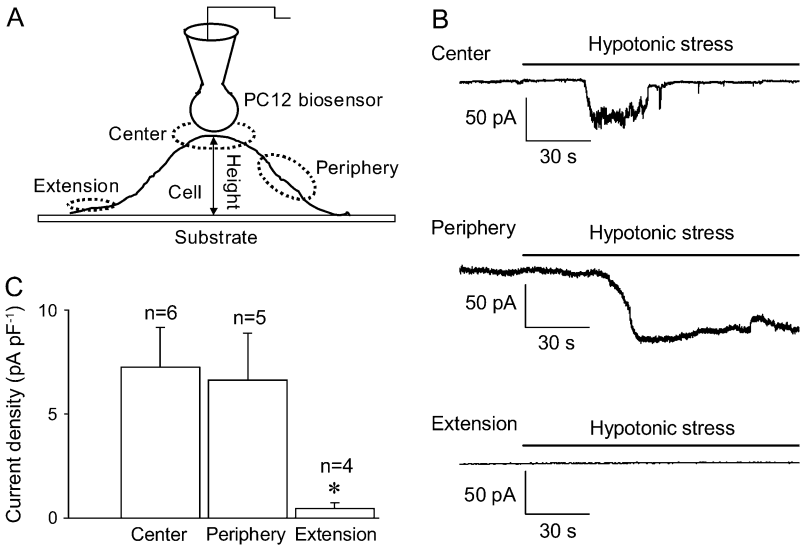

FIGURE 3 Swelling-induced release of ATP from different regions of the sarcolemma of cultured rat cardiomyocytes. (*A*) Diagram representing the position of the biosensor cell on the sarcolemma of a rat cardiomyocyte. (*B*) Representative current records obtained from a voltage-clamped (at −50 mV) PC12 cell placed on the central (*top trace*), peripheral (*middle trace*) and extension (*bottom trace*) regions of a cultured neonatal rat cardiomyocyte. (*C*) Summarized peak current responses evoked by swelling-induced ATP release from cultured cardiomyocytes. Each column represents the mean ± SE (vertical bar). $*p < 0.05$ vs. center.

Maxi-anion channels in adult rat cardiomyocytes monitored by conventional patch-clamp

It was reported previously that maxi-anion channels are only transiently expressed in neonatal rat cardiomyocytes and could not be found in adult cells (15). Indeed, when patched by a conventional method using relatively large pipettes (~2 MΩ when filled with the experimental pipette solutions), only an indiscriminate rise in the patch conductance, without the specific pattern of maxi-anion channel activity, was observed in 2 experiments of 11 attempts (18%, data not shown). Recent studies have suggested that several types of other ion channels can be specifically targeted to the T-tubular system of cardiomyocytes (19,22,26). Therefore, we hypothesized that the failure to observe functional maxi-anion channels in adult cells in previous studies (14,15) was due to the specific localization of the maxi-anion channel. To test this hypothesis we used patch pipettes with finer tips (15–20 MΩ) and targeted only areas of Z-lines visible under a light microscope at high magnification, in cardiomyocytes freshly isolated from adult rat hearts. The membrane patches formed were silent in the cell-attached mode (Fig. 4 *A*). However,

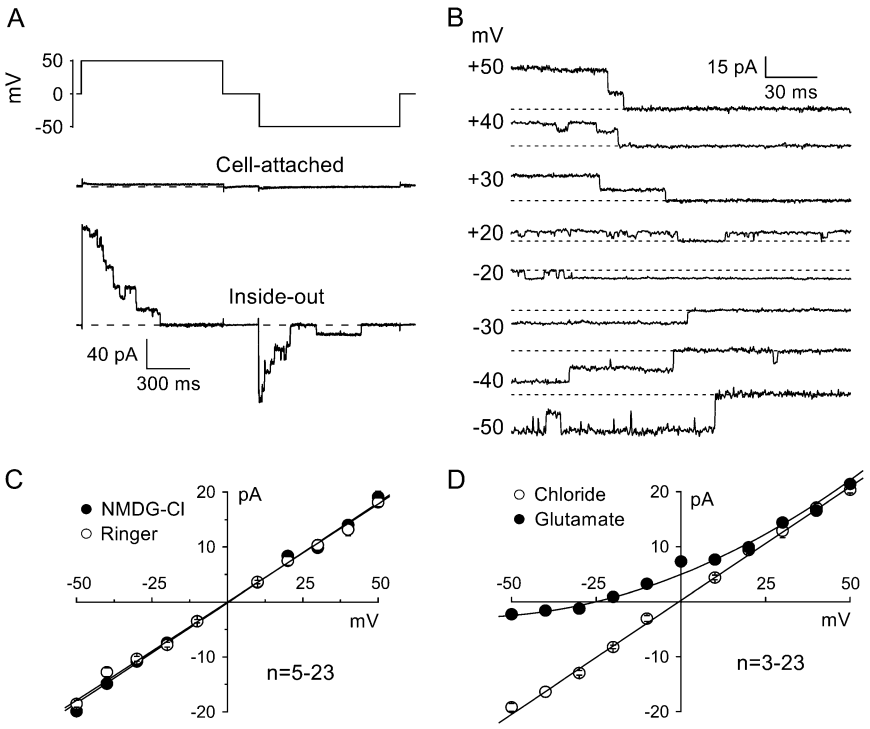

FIGURE 4 Functional expression of maxi-anion channel in the sarcolemma of freshly isolated adult rat cardiomyocytes. (*A*) Representative traces of single-channel currents recorded in the cell-attached mode (*upper trace*) and after patch excision (*lower trace*), in response to step pulses to ±50 mV (the protocol is shown at the top of the traces). Dotted lines indicate the zero current level. (*B*) Representative current traces showing single-channel events at different voltages (given on the left of each trace). The dotted lines indicate the closed state. (*C*) I/V relationship for maxi-anion channel currents recorded with Ringer solution (*open symbols*) or NMDG-Cl solution (*solid symbols*) in the bath. Pipette contained TEA-Cl solution. Each symbol represents the mean amplitude of unitary currents with mean ± SE (*vertical bar*). (*D*) Effect of anion substitution on the single-channel I/V relationship in inside-out patches. Currents were recorded in control Cl^--rich conditions in which bath and pipette contained Ringer solution (*open circles*), or in glutamate-rich conditions in which the NaCl of the bath Ringer solution was replaced with Na-glutamate (*solid circles*). The solid line is a polynomial fit with the reversal potential indicated in the text. Each symbol represents the mean value with mean ± SE (*vertical bar*).

patch excision in 11 experiments of 19 attempts (58%: significantly different from the incidence of indiscriminate conductance increase observed with 2 MΩ-pipettes) resulted in activation of maxi-channel events (Fig. 4 *A*, *bottom trace*) with properties similar to those seen in neonatal cells. The channels showed voltage-dependent inactivation at potentials greater than ±20 mV (Fig. 4, *A* and *B*). The unitary current-voltage (I/V) relationship of the fully open channel was linear with a unitary slope conductance of 365.5 ± 6.5 pS, and the reversal potential was ~0 mV, as shown in Fig. 4 *C* (*open circles*). Neither the shape of the unitary I/V relationship nor the reversal potential changed when monovalent cations in the bath were replaced with $NMDG^+$ (*solid circles*). In contrast, replacement of Cl^- with $glutamate^-$ in the bath solution shifted the reversal potential to a value of −29.7 ± 1.2 mV (Fig. 4 *D*). This result indicates that the maxi-anion channel in adult cells is anion-selective with a permeability ratio of $glutamate^-$ to Cl^- of 0.26 ± 0.02.

Fig. 5 illustrates the basic pharmacology of the adult cardiomyocyte maxi-anion channels activated after excision. In our experiments, a carboxylate analog Cl^- channel blocker, NPPB (100 μM), prominently decreased the single-channel amplitude in symmetrical Cl^- conditions. A stilbene-derivative Cl^- channel blocker, SITS (100 μM), blocked inside-out single-channel events. Arachidonic acid (10 μM), a potent blocker of the maxi-anion channel (6), also inhibited activity of the channel observed in the inside-out mode. Effects of these drugs on the mean amplitude of patch currents activated after excision are summarized in Fig. 5 *B*. Consistent with our previous observations (5,14), bath (intracellular) application of Gd^{3+} (50 μM) failed to block the channel activity in inside-out patches. In our experiments we failed to obtain outside-out patches due to the very small size of the pipette tips. Instead, we added 50 μM Gd^{3+} into the pipette solution and tested the effect of extracellular Gd^{3+} on the maxi-anion channel activity after patch excision. Gd^{3+} in the pipette completely abolished the channel activity in adult rat cardiomyocytes in 11 experiments (data not shown, channel incidence 0%: significantly different from the incidence in Z-line-targeted pipettes filled with control solution).

Maxi-anion channels in adult rat cardiomyocytes monitored by a smart-patch technique

The Z-lines could be clearly distinguished in cardiomyocytes freshly isolated from adult rats by phase-contrast microscopy (Fig. 6 *A*). In the following experiments, we narrowed the area for scanning by patch pipette to $\sim 10 \times 10\ \mu m^2$. Fig. 6 *B* shows a representative topographic SICM image of the cell surface of an adult rat cardiomyocyte, obtained using a very fine-tipped capillary pipette that had a resistance of 80–100 MΩ when filled with experimental pipette solution. In this image, Z-grooves, scallop crests, and the openings of transverse tubules (T-tubules) are clearly visible. The Z-Z distance could be estimated from the profile of the surface height along a line drawn perpendicular to the Z-lines (Fig. 6 *C*). The average Z-Z distance in our experiments was 2.01 ± 0.05 μm ($n = 24$ from 15 different cells). This figure is very similar to that obtained by immunocytochemistry (26,27) and by scanning ion conductance microscopy in low-Ca^{2+} solution (20,22,23) and in standard Ringer solution containing 1.5 mM Ca^{2+} (28). When we attempted to patch the sarcolemma using these very fine pipettes, we observed channel activity only on very rare occasions. Therefore, in the following experiments, to increase the membrane area to be patched, we used pipettes with slightly larger openings with tip resistance of 20–35 MΩ. Although the resolution of the images dropped in these experimental conditions, Z-grooves, scallop crests, and the openings of T-tubules were clearly visible (Fig. 6 *D*). The estimated Z-Z distance (Fig. 6 *E*) in these conditions was 2.11 ± 0.09 μm ($n = 36$ from 15 different cells) and very similar to the result obtained with very fine pipettes.

In the following experiments, we used the same pipettes to patch different areas of the sarcolemma after taking 3D images. Single-channel events of 17.9 ± 1.0 pA at +50 mV and 17.7 ± 1.0 pA at –50 mV were recorded from patches excised from

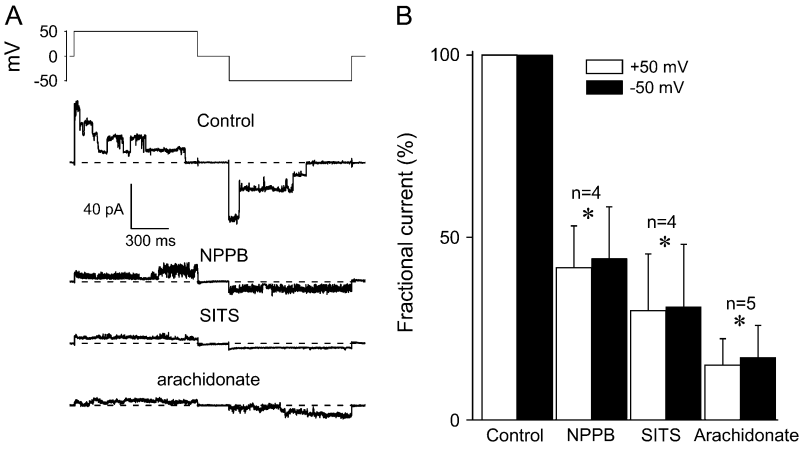

FIGURE 5 Pharmacologic profile of maxi-anion channels in freshly isolated adult rat cardiomyocytes. (*A*) Representative current traces with single-channel events recorded during application of step pulses (the protocol is shown at the top of the traces) from excised inside-out patches in the absence (*control*) or presence of drugs. The drugs used were NPPB (100 μM), SITS (100 μM), and arachidonic acid (10 μM). Dotted lines indicate the zero current level. (*B*) Effects of drugs on mean currents for excised inside-out patches. Currents were recorded at +50 mV (*open columns*) and −50 mV (*solid columns*). Data are normalized to the mean current measured before application of drugs and are corrected for background currents. Each column represents the mean ± SE (*vertical bar*). *$p <$ 0.05 vs. control.

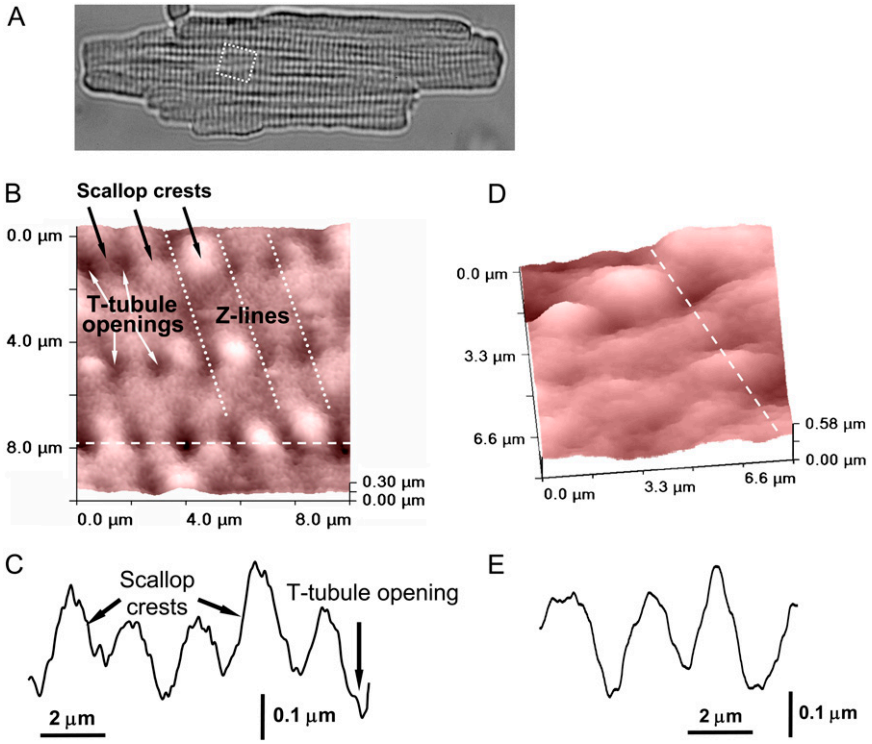

FIGURE 6 Freshly isolated adult rat cardiomyocytes imaged by SICM. (*A*) Optical image of freshly isolated adult rat cardiomyocytes. (*B*) Representative topographic image of a rat cardiomyocyte obtained using a fine nanopipette (90 MΩ, when filled with pipette solution). Z-grooves, T-tubule openings, and scallop crests are indicated. (*C*) Variation of the cell height along a line drawn as indicated by dashed white line in (*B*). (*D*) Representative topographic image of a rat cardiomyocyte obtained using a relatively wide-tipped micropipette (35 MΩ). (*E*) Variation of the cell height along a line drawn as indicated by dashed white line.

T-tubule openings (Fig. 7 *A, left panel*). Similarly, single-channel currents of 18.4 ± 1.5 pA at +50 mV and −19.1 ± 0.8 pA at −50 mV were recorded in patches excised from Z-grooves (Fig. 7 *A, center panel*). These channels had linear current-voltage relationships with slope conductances of 344 ± 9.0 pS and 370.1 ± 8.8 pS for T-tubule openings and Z-lines, respectively (Fig. 7 *B*). In contrast, the activity of maxi-anion channels in the scallop crest was very low (Fig. 7 *A, right panel*) and was observed in only one of 14 patches tested. The mean NP_o value was significantly lower for scallop crests compared with T-tubule openings and Z-grooves (Fig. 7 *C*). These results indicate that the maxi-anion channel is expressed predominantly in T-tubule openings and Z-grooves.

Swelling-induced activation of maxi-anion channels and ATP release in adult rat cardiomyocytes

In the cell-attached (on-cell) configuration, single-channel events were rarely observed in adult cardiomyocytes perfused with isotonic solution. When the isotonic bath solution was replaced with hypotonic solution, we could observe, even in the giga-sealed cell-attached configuration, single-channel events of large amplitude after a lag period of 9.2 ± 2.8 min ($n = 5$) (Fig. 8 *A*). The mean amplitudes of single-channel events were 17.5 ± 1.0 pA ($n = 9$) and −7.5 ± 0.3 pA ($n = 7$) at holding potentials (−Vp) of +50 and −50 mV, respectively (Fig. 8 *B*). The unitary I/V relationship for single-channel events exhibited outward rectification (Fig. 8 *C*), presumably due to a lower Cl^- concentration within the cell. A PC12 biosensor cell was placed in close proximity to (often touching) the surface of isolated adult rat cardiomyocytes and whole-cell currents were recorded to measure the local concentration of ATP released. On exposure to a hypotonic stimulation, inward current spikes were recorded from the PC12 cell touching the top of the isolated adult rat cardiomyocytes with a lag period of 2.4 ± 0.8 min ($n = 4$), as shown in Fig. 8 *D*. The mean peak current density was 6.6 ± 2.3 pA/pF ($n = 4$), which corresponds to a local ATP concentration of 18.7 ± 7.0 μM. Swelling-induced ATP release detected by the biosensor was largely abolished by the presence of 100 μM NPPB in the bath (Fig. 8 *D*, $n = 4$). No ATP-evoked inward current response was detected by the biosensor when the cardiomyocytes were exposed to isotonic high-K^+ bath solution for 5 to 10 min ($n = 3$), indicating that depolarization per se does not induce the ATP release.

DISCUSSION

In our experiments, we used the technique developed recently of scanning ion conductance microscopy and a smart-patch method to investigate the spatial distribution of maxi-anion channels on the sarcolemmal surface. Cellular extensions located in the region within 20% from the bottom of the cell exhibited significantly lower maxi-anion channel activity compared with the other (central and peripheral) parts of the cell body. Interestingly, the efficiency of local ATP release, tested using the biosensor technique, also showed a strikingly

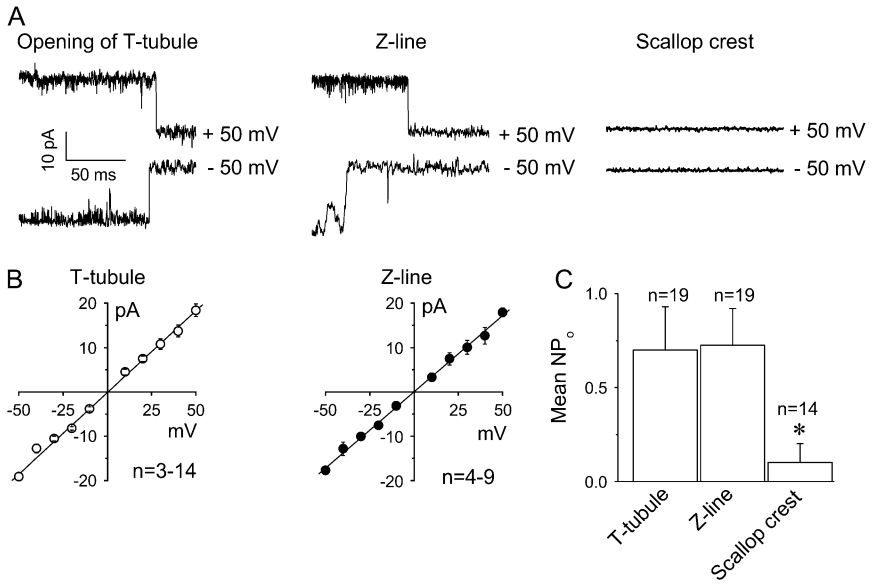

FIGURE 7 Maxi-anion channel activity in patches excised from different zones of freshly isolated rat cardiomyocytes using the smart-patch technique. (*A*) Representative single-channel events recorded at +50 mV (*upper traces*) and −50 mV (*lower traces*) in the opening of a T-tubule, in the Z-line, and on the scallop crest. (*B*) Current-voltage relationships for the maxi-anion channel currents recorded in the openings of T-tubules and in the Z-grooves. Each symbol represents the mean value with mean ± SE (*vertical bar*). (*C*) Mean maxi-anion channel activity (expressed as NP_o) in the different regions of the sarcolemma of isolated adult rat cardiomyocytes. Each column represents the mean ± SE (*vertical bar*). $*p < 0.05$ vs. opening of T-tubule.

similar pattern. This result underscores the relationship between the maxi-anion channel and the ATP release pathway (2,4). In our preliminary experiments, the distribution of another anion channel, the volume-sensitive outwardly rectifying (VSOR) Cl^- channel, did not show any difference among these three areas (A. Dutta, Y. Okada, and R. Z. Sabirov, unpublished data), suggesting that cell extensions do not generally exhibit different patterns of the channel expression.

The transverse tubules (T-tubules) of mammalian cardiac ventricular myocytes are invaginations of the surface membrane that occur at the Z-line and have both transverse and longitudinal elements (26). Many of the proteins, including voltage-gated L-type Ca^{2+} channels (29), involved in excitation-contraction coupling seem to be concentrated at T-tubules. Using the SICM technique, Korchev et al. (19) showed directly that ATP-sensitive potassium (K_{ATP}) channels are also clustered near the openings of T-tubules. Gu et al. (22) used the same technique to record L-type Ca^{2+} channels and three different chloride channels with intermediate unitary conductances at the openings of T-tubules. We thus hypothesized that the ATP-conductive maxi-anion channel might also be targeted to the same region.

The SICM method is very effective in resolving fine structures on the surface of cells and was used to patch the sarcolemma in the area of Z-lines of cardiac cells (19,22,28). In our study, we used this smart-patch technique and obtained images of the adult cardiomyocyte cell surface with a Z-Z distance of ~2 μm, a value that is very similar to the values reported

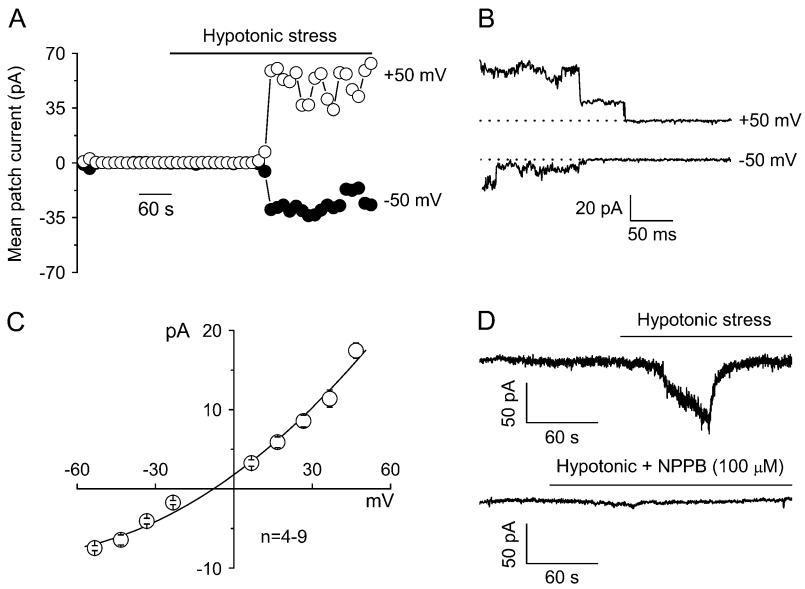

FIGURE 8 Maxi-anion channel and ATP release activities induced by hypotonic stress in adult rat cardiomyocytes. (*A*) Representative mean patch currents recorded during application of alternating pulses from 0 to ±50 mV (every 10 s) in a cell-attached patch before and during (*horizontal bar*) exposure to hypotonic solution. (*B*) Representative current traces with single-channel events occurring in response to step pulses to ±50 mV in a cell-attached patch. (*C*) Unitary I/V relationship for single-channel events recorded from cell-attached patches. Each symbol represents the mean amplitude of unitary currents with mean ± SE (*vertical bar*). (*D*) Representative trace of biosensor current activated in response to swelling-induced ATP release from an adult rat cardiomyocyte. Whole-cell currents were recorded from a PC12 cell while positioning it in contact with an adult cardiomyocyte before and during (*horizontal bar*) application of hypotonic solution with no drug added (*upper trace*) and in the presence of 100 μM NPPB (*lower trace*).

previously (26). Using fine-tipped nanopipettes, we patched different regions of the cell surface and found that channel activity was maximal at the openings of T-tubules and along Z-lines, and significantly less in the scallop crest area. Based on these results, we conclude that the distribution pattern of the maxi-anion channel parallels the expression pattern of other ion channels involved in the excitation of cardiac myocytes, such as voltage-gated Ca^{2+} channels, and K_{ATP} channels. The T-tubular system is known to be absent in neonatal cells and to disappear with continuous culturing of adult cells (26). When adult cardiomyocytes exhibiting a well-developed T-tubular system are patched with conventional 2-MΩ-pipettes, the complex shape of the T-tubular system might facilitate the formation of closed vesicle-like structures that distort the measured ionic currents through maxi-anion channels. This would result in poorly resolved records, as actually observed in our experiments (data not shown). The lack of a T-tubular system may explain why maxi-anion channels are accessible to pipettes in conventional patch-clamp experiments with primary cultured neonatal cardiomyocytes.

The specific localization of maxi-anion channels at the openings of T-tubules and along Z-lines implies that the stimulated release of ATP is also localized around these regions, although the relatively large size of the biosensor cells (~10 μm) compared with that of the T-tubule openings (~2 μm) did not allow precise determination of the ATP-releasing site on the surface of adult cardiomyocytes. However, it is notable that using a biosensor technique, sizable ATP release was not detected at the lateral end, which corresponds to the intercalated disk lacking T-tubule openings, of freshly isolated adult rat cardiomyocytes (A. K. Dutta, unpublished data).

The major constituent of the swelling-activated chloride conductance in cardiomyocytes is the volume-sensitive outwardly rectifying (VSOR) Cl^- channel (30–34) with properties similar to those reported for epithelial and other cell types (35). In our previous study we have shown that the mass ATP release from cultured neonatal cardiomyocytes requires only brief opening of a small number of maxi-anion channels (14). It is conceivable that this inference is also valid for freshly isolated cardiomyocytes from adult animals. We therefore suppose that brief activation of few maxi-anion channels alone is not sufficient to affect the total membrane conductance observed in whole-cell recordings from cardiomyocytes under hypotonic stress. The mean NP_o values obtained in recordings from T-tubules and Z-lines in experiments with adult cardiomyocytes (Fig. 7 *C*) were about half of the values obtained from center and periphery area of cultured neonatal cells (Fig. 2 *D*). This may suggest that the local channel density at T-tubules and Z-lines of adult cells is two times lower compared with neonatal cells. Given that T-system may occupy 20–60% of the total surface of sarcolemma (26), probability of detection of the maxi-anion channel event by whole-cell recordings in freshly isolated adult cells is expected to be substantially lower compared with the cultured neonatal cells.

In the on-cell mode, the average lag time for channel activation (~9.2 min: Fig. 8 *A*) was longer compared with that for ATP-evoked biosensor currents (~2.4 min: Fig. 8 *D*). This apparent discrepancy could be due to a complex shape of the membrane patches containing fragments of the T-system. In addition, the channels in the cell-attached patch membrane are spatially separated by a giga-sealed patch pipette from the rest of plasma membrane, which actually receives the stimuli, and therefore a longer time lag was necessary for the signals to reach the maxi-anion channel in the patch membrane. Mechanical perturbation due to giga-seal formation should also be taken into account, because the lag time for swelling-induced activation of maxi-anion channels in the loose-patch on-cell configuration was much shorter than that in the giga-seal on-cell configuration and even shorter than the lag time for ATP release response detected by the biosensor technique (14). Possible upregulation of the maxi-anion channel by released external ATP, in an autocrine positive-feedback fashion, could also fasten ATP release detected by the biosensor but not activation of maxi-anion channel recorded in the cell-attached patch to which released ATP cannot reach. The precise mechanism of maxi-anion channel activation on osmotic and ischemic stimulation as well as on patch excision remains unknown and is currently under investigation in our laboratory.

The functional significance of the localization of maxi-anion channels to the Z-grooves and T-tubules can be considered in two different aspects. First is the direct effect of the increased chloride conductance on the local membrane potential around T-tubules, and second is the effect mediated by ATP release. The maxi-anion channel activation is expected to produce repolarizing outward current by Cl^- influx, and therefore may be involved in maintaining the T-tubule membrane potential. This repolarizing effect should be particularly important during ischemia, because ischemia-induced sustained activation of ATP-sensitive K^+ channels will cause potassium accumulation due to a limited diffusion of K^+ ions in the T-tubules (36), thereby resulting in depolarization of T-tubule.

The maxi-anion channel has a unique property to conduct ATP. Cardiomyocytes do release ATP, and we have provided compelling evidence for the involvement of the maxi-anion channel in this process using cultured neonatal cardiomyocytes (14). Extracellular ATP is known to be protective during ischemic preconditioning, possibly via activation of p38 MAPK (8). The results of our study may suggest that maxi-anion channel-mediated purinergic signaling is confined to the T-tubular system, although the spatial distribution of P2 receptors over the surface of cardiomyocytes remains poorly investigated.

In summary, we succeeded not only in showing, for the first time, functional expression of the maxi-anion channel on the plasma membrane of adult rat cardiomyocytes, but also in observing spatial distribution of the maxi-anion channel over the surface of both adult and neonatal rat cardiomyocytes by applying a smart-patch technique. In addition, spatial

distribution of the ATP-releasing site was found to essentially match with that of the maxi-anion channel in neonatal cardiomyocytes by using an ATP biosensor technique. This fact provides additional evidence supporting the maxi-anion channel = ATP-conductive channel concept.

The authors thank E.L. Lee for manuscript preparation, T. Shimizu for discussion, and T. Okayasu for secretarial help as well as M. Ohara, K. Shigemoto, and A. Toychiev for technical assistance.

This work was supported by Grants-in-Aid for Scientific Research (A) and (C) to Y.O. and R.Z.S. from the Ministry of Education, Culture, Sports, Science and Technology of Japan, by a grant from Salt Science Foundation to Y.O., by a grant from the Japan Society for Promotion of Science (JSPS) to A.K.D. and by the Biotechnology and Biological Sciences Research Council (Y.E.K. and A.I.S.).

REFERENCES

1. Strange, K., F. Emma, and P. S. Jackson. 1996. Cellular and molecular physiology of volume-sensitive anion channels. *Am. J. Physiol.* 270:C711–C730.
2. Sabirov, R. Z., and Y. Okada. 2005. ATP release via anion channels. *Purinergic Signal.* 1:311–328.
3. Sabirov, R. Z., and Y. Okada. 2004. Wide nanoscopic pore of Maxi-anion channel suits its function as an ATP-conductive pathway. *Biophys. J.* 87:1672–1685.
4. Sabirov, R. Z., and Y. Okada. 2004. ATP-conductive maxi-anion channel: a new player in stress-sensory transduction. *Jpn. J. Physiol.* 54:7–14.
5. Sabirov, R. Z., A. K. Dutta, and Y. Okada. 2001. Volume-dependent ATP-conductive large-conductance anion channel as a pathway for swelling-induced ATP release. *J. Gen. Physiol.* 118:251–266.
6. Dutta, A. K., Y. Okada, and R. Z. Sabirov. 2002. Regulation of an ATP-conductive large-conductance anion channel and swelling-induced ATP release by arachidonic acid. *J. Physiol.* 542:803–816.
7. Bell, P. D., J. Y. Lapointe, R. Sabirov, S. Hayashi, J. Peti-Peterdi, K. Manabe, G. Kovacs, and Y. Okada. 2003. Macula densa cell signaling involves ATP release through a maxi anion channel. *Proc. Natl. Acad. Sci. USA.* 100:4322–4327.
8. Vassort, G. 2001. Adenosine 5′-triphosphate: a P2-purinergic agonist in the myocardium. *Physiol. Rev.* 81:767–806.
9. Burnstock, G., and C. Kennedy. 1986. Purinergic receptors in the cardiovascular system. *In* Receptors in the Cardiovascular System. Progress in Pharmacology, Vol. 6, No. 2. P. A. van Zwieten and E. Schönbaum, editors. Gustav Fischer Verlag, Stuttgart, Germany. 111–132.
10. Pelleg, A., C. M. Hurt, and E. L. Michelson. 1990. Cardiac effects of adenosine and ATP. *Ann. N. Y. Acad. Sci.* 603:19–30.
11. Burnstock, G. 1972. Purinergic nerves. *Pharmacol. Rev.* 24:509–581.
12. Sparks, H. V., Jr., and H. Bardenheuer. 1986. Regulation of adenosine formation by the heart. *Circ. Res.* 58:193–201.
13. Forrester, T., and C. A. Williams. 1977. Release of adenosine triphosphate from isolated adult heart cells in response to hypoxia. *J. Physiol.* 268:371–390.
14. Dutta, A. K., R. Z. Sabirov, H. Uramoto, and Y. Okada. 2004. Role of ATP-conductive anion channel in ATP release from neonatal rat cardiomyocytes in ischaemic or hypoxic conditions. *J. Physiol.* 559: 799–812.
15. Coulombe, A., and E. Coraboeuf. 1992. Large-conductance chloride channels of new-born rat cardiac myocytes are activated by hypotonic media. *Pflugers Arch.* 422:143–150.
16. Simpson, P., and S. Savion. 1982. Differentiation of rat myocytes in single cell cultures with and without proliferating nonmyocardial cells. Cross-striations, ultrastructure, and chronotropic response to isoproterenol. *Circ. Res.* 50:101–116.
17. Wolska, B. M., and R. J. Solaro. 1996. Method for isolation of adult mouse cardiac myocytes for studies of contraction and microfluorimetry. *Am. J. Physiol.* 271:H1250–H1255.
18. Korchev, Y. E., M. Milovanovic, C. L. Bashford, D. C. Bennett, E. V. Sviderskaya, I. Vodyanoy, and M. J. Lab. 1997. Specialized scanning ion-conductance microscope for imaging of living cells. *J. Microsc.* 188:17–23.
19. Korchev, Y. E., Y. A. Negulyaev, C. R. Edwards, I. Vodyanoy, and M. J. Lab. 2000. Functional localization of single active ion channels on the surface of a living cell. *Nat. Cell Biol.* 2:616–619.
20. Gorelik, J., Y. Gu, H. A. Spohr, A. I. Shevchuk, M. J. Lab, S. E. Harding, C. R. Edwards, M. Whitaker, G. W. Moss, D. C. Benton, D. Sanchez, A. Darszon, I. Vodyanoy, D. Klenerman, and Y. E. Korchev. 2002. Ion channels in small cells and subcellular structures can be studied with a smart patch-clamp system. *Biophys. J.* 83:3296–3303.
21. Gorelik, J., Y. Zhang, A. I. Shevchuk, G. I. Frolenkov, D. Sanchez, M. J. Lab, I. Vodyanoy, C. R. Edwards, D. Klenerman, and Y. E. Korchev. 2004. The use of scanning ion conductance microscopy to image A6 cells. *Mol. Cell. Endocrinol.* 217:101–108.
22. Gu, Y., J. Gorelik, H. A. Spohr, A. Shevchuk, M. J. Lab, S. E. Harding, I. Vodyanoy, D. Klenerman, and Y. E. Korchev. 2002. High-resolution scanning patch-clamp: new insights into cell function. *FASEB J.* 16: 748–750.
23. Shevchuk, A. I., J. Gorelik, S. E. Harding, M. J. Lab, D. Klenerman, and Y. E. Korchev. 2001. Simultaneous measurement of Ca^{2+} and cellular dynamics: combined scanning ion conductance and optical microscopy to study contracting cardiac myocytes. *Biophys. J.* 81:1759–1764.
24. Hazama, A., S. Hayashi, and Y. Okada. 1998. Cell surface measurements of ATP release from single pancreatic β cells using a novel biosensor technique. *Pflugers Arch.* 437:31–35.
25. Hayashi, S., A. Hazama, A. K. Dutta, R. Z. Sabirov, and Y. Okada. 2004. Detecting ATP release by a biosensor method. *Sci. STKE.* 258:pl 14.
26. Brette, F., and C. Orchard. 2003. T-tubule function in mammalian cardiac myocytes. *Circ. Res.* 92:1182–1192.
27. Scriven, D. R., P. Dan, and E. D. Moore. 2000. Distribution of proteins implicated in excitation-contraction coupling in rat ventricular myocytes. *Biophys. J.* 79:2682–2691.
28. Duclohier, H. 2005. Neuronal sodium channels in ventricular heart cells are localized near T-tubules openings. *Biochem. Biophys. Res. Commun.* 334:1135–1140.
29. Brandt, N. R., R. M. Kawamoto, and A. H. Caswell. 1985. Dihydropyridine binding sites on transverse tubules isolated from triads of rabbit skeletal muscle. *J. Recept. Res.* 5:155–170.
30. Hagiwara, N., H. Masuda, M. Shoda, and H. Irisawa. 1992. Stretch-activated anion currents of rabbit cardiac myocytes. *J. Physiol.* 456:285–302.
31. Hiraoka, M., S. Kawano, Y. Hirano, and T. Furukawa. 1998. Role of cardiac chloride currents in changes in action potential characteristics and arrhythmias. *Cardiovasc. Res.* 40:23–33.
32. Gong, W., H. Xu, T. Shimizu, S. Morishima, S. Tanabe, T. Tachibe, S. Uchida, S. Sasaki, and Y. Okada. 2004. ClC-3-independent, PKC-dependent activity of volume-sensitive Cl^- channel in mouse ventricular cardiomyocytes. *Cell. Physiol. Biochem.* 14:213–224.
33. Duan, D. Y., L. L. Liu, N. Bozeat, Z. M. Huang, S. Y. Xiang, G. L. Wang, L. Ye, and J. R. Hume. 2005. Functional role of anion channels in cardiac diseases. *Acta Pharmacol. Sin.* 26:265–278.
34. Baumgarten, C. M., D. M. Browe, and Z. Ren. 2005. Swelling- and stretch-activated chloride channels in the heart: regulation and function. *In* Mechano-Electric Feedback in the Heart: Fundamental and Clinical Aspects. A. Kamkin and I. Kiseleva, editors. Academic Book, Moscow. 79–102.
35. Okada, Y. 1997. Volume expansion-sensing outward rectifier Cl channel: a fresh start to the molecular identity and volume sensor. *Am. J. Physiol. Cell Physiol.* 273:C755–C789.
36. Swift, F. T., A. Stromme, B. Amundsen, O. M. Sejersted, and I. Sjaastad. 2006. Slow diffusion of K^+ in the T tubules of rat cardiomyocytes. *J. Appl. Physiol.* 101:1170–1176.